

FULL PAPER

Open Access



Reachable set analysis of practical trans-lunar orbit via a retrograde semi-analytic model

Bo-yong He^{*} , Sheng-gang Wu and Heng-nian Li

Abstract

Different from the Apollo flight mode, a safer trans-lunar flight mode for the crews is preferred. The previous-arrived lunar module rendezvouses with the crew exploration vehicle at a low lunar destination orbit, and then the crews ride the lunar module to descend the lunar surface sampling destination. The lunar module, which includes the descent and ascent stages, flies from a low Earth orbit to the low lunar destination orbit with two tangential impulses. The low lunar destination orbital reachable set of the practical trans-lunar orbit limits the feasible lunar surface sampling region. Therefore, this paper addresses the low lunar destination orbital reachable set of the practical trans-lunar orbit. A retrograde semi-analytic model is proposed for rapidly computing the practical two-impulse trans-lunar orbit firstly, which refers the ephemeris table twice for more precision perilune orbital elements. The reachable set is generated using the multiple-level traversal searching approach with this retrograde semi-analytic mode. Its envelope is re-checked by the continuation theory with the high-precision orbital model. Besides, some factors that affect the reachable set are also measured. The results show that neither the Earth–Moon distance nor the trans-lunar duration affects the reachable set. However, if the trans-lunar injection inclination is smaller than the inclination of the moon's path, the reachable set becomes smaller or even reduces into an empty set. In brief, the proposed retrograde semi-analytic model for computing the reachable set provides a helpful and fast tool for selecting an applicable lunar surface sampling site for the manned lunar mission overall design.

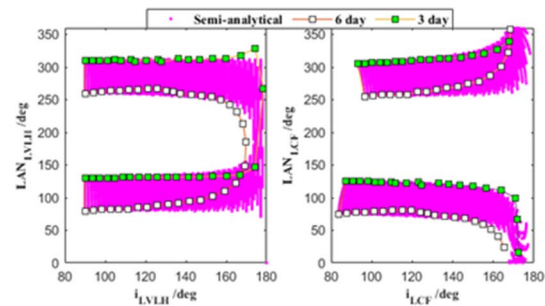
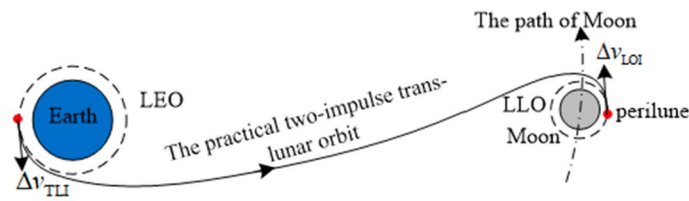
Keywords Manned lunar mission, Trans-lunar orbit, reachable set, Semi-analytical, Two-impulse

*Correspondence:

Bo-yong He
heboyong@yeah.net

Full list of author information is available at the end of the article

Graphical Abstract



This paper demonstrates a retrograde semi-analytic model to rapidly compute the lunar approach orbital plane reachable set (i.e., the inclination and the longitude of ascending node) of the practical two-impulse trans-lunar orbit of the lunar module for the safer manned lunar mission based on lunar orbit rendezvous. The helpful and fast tool are re-checked with the high-precision model. Some factors that affect the reachable set are also measured. It provides the basic theoretical basis for lunar surface sampling selection.

Introduction

The moon as the nearest celestial body is also the compulsory training camp for human's interstellar travels. After the *Apollo project*, especially when the evidences of water in lunar south pole are discovered by many lunar polar orbiters (Colaprete et al. 2010), new plans for the manned lunar mission by USA and other countries have become more diverse. The National Aeronautics and Space Administration (NASA) have published three important reports on the *Constellation Program* after 2005 (Stanley et al. 2005; Condon 2007; Garn et al. 2008). Although the *Constellation Program* was replaced later by the *Lunar Orbital Platform-Gateway Program* (Davis 2018), the aims of lunar *Global Access* and *Any-time Return* remained unchanged. Different from the lunar low latitude area detection of the *Apollo project*, the lunar polar and high-latitude districts would be the next manned lunar mission destination for water and possible lunar life. In the *Constellation Program*, NASA proposed a new idea called *crew and cargo separation* that the lunar module (i.e., descend and ascend stages are merged) transferred to a low lunar orbit (LLO) by a practical trans-lunar duration about 4–5 day, to wait for a crew exploration vehicle for rendezvous and assembling. Compared with the *Apollo flight mode*, this new flight mode is safer for crews (Stanley et al. 2005). When it comes to the mode of a 3-day trans-lunar orbit used in the *Apollo Project*, the new mode is also more fuel-saving for trans-lunar injection (TLI) and low lunar orbit insertion (LOI) (He and Shen 2020). To save fuel, TLI and LOI are hoped to be tangential to the periapsis velocity vector. With the two constraints (i.e., the trans-lunar duration and tangential velocity increments), the orbital elements reachable set of LLO for the lunar module rendezvous with the

crew exploration vehicle becomes a significant factor to select a feasible lunar surface sampling site. Therefore, this paper studies the reachable set of the practical two-impulse trans-lunar orbits.

In February 1959, the Luna-1 lunar impact probe launched by Soviet Union did not reach the goal of hitting the lunar surface because of its inaccurate trans-lunar orbital dynamics model and designed method. The Luna-2, launched in September 1959, successfully hit the lunar surface and became the first human lunar probe. After that, dozens of lunar probes including the unmanned and manned cases have had successfully missions to the Moon. However, the well-known trans-lunar orbital dynamics models could be divided into only four items, namely, the circular restricted three-body problem (CR3BP), the double two-body model, the pseudo-state model, and the high-precision model. *Issac Newton* described the CR3BP in his *Philosophiae Naturalis Principia Mathematica*, which shows the mathematical formulas of the orbits in a three-body system. CR3BP still need numerical integration (Lee et al. 2014). The double two-body model was proposed based on the principle of computing the celestial body's gravitational sphere in the *Pierre Simon Laplace's* monumental work *Celestial Mechanics* (Egorov 1958). Wilson (1970) and Byrnes and Hooper (1970) proposed the pseudo-state model around 1970s. It is also named the multi-conic method. It calculates a trans-lunar orbit using both the Earth's and the Moon's gravitational forces acting on the spacecraft gradually. Such calculation consumes about 1% of the numerical integration time, and its model errors are no more than 5% compared with the double two-body model. The perilune attitude error for a trans-lunar

orbit is about 20 km (Zhou et al. 2019). Apart from the above trans-lunar orbital dynamical models, the high-precision model considers all the known perturbation forces acting on the spacecraft. Thus, it is the most accurate dynamic model that reflects the real scenario with a huge potential in the near future (Yan and Gong 2011). To design a trans-lunar orbit with a high-precision model, a simplified orbital model is applied usually to provide an initial value of the design variable (Mohammad and Roberto 2019). The double two-body model is selected usually to play the role of the simplified orbital model because of its semi-analytical feature. However, the selections of the parameters are different. Peng et al. (2011) and Gao et al. (2018) selected the entry point parameters on the lunar influence sphere to play the orbital patched conic parameters. Li et al. (2015) selected the exit point parameters to do this. The above orbital patched conic techniques that select the entry or exit point are difficult to compute the precision orbital position and velocity at the epochs of the perilune and perigee. Because they referred the Jet Propulsion Laboratory (JPL) ephemeris table for the Moon's position and velocity at the epochs of the entry or exit point, but ignore the Moon's position and velocity deviations when the spacecraft flies inside the Moon's gravitational influence sphere. And the Lambert iteration is needed to compute the orbital elements in the Earth-centric segment, so its calculation efficiency is low. A set of the perilune parameters selected in our previous works (He et al. 2019) is an effective measure for avoiding the orbital perilune-state deviation.

The reachable set of non-linear differential equations refers to the dynamic system as Eq. (1). If the system is consecutive within $t \in [t_0, t_f]$, and there is an initial state set $\mathbf{x}(t_0) \in \Theta^n \subseteq \mathbf{R}^n$ at the moment t_0 . There exists a control set $\mathbf{u}(t) \in \mathbf{U}^m \subseteq \mathbf{R}^n$ that causes the final state $\mathbf{x}(t_f) \in \Omega^n \subseteq \mathbf{R}^n$ at the moment t_f , then the Ω^n can be called the reachable set of the initial set Θ^n (Grantham. 1981).

$$\begin{cases} \dot{\mathbf{x}}(t) = \mathbf{f}[t, \mathbf{x}(t), \mathbf{u}(t)] \\ \mathbf{y}(t) = \mathbf{c}[t, \mathbf{x}(t)] \\ \mathbf{x}(t_0) \in \Theta^n, \mathbf{u}(t) \in \mathbf{U}^m, \mathbf{y}(t_f) \in \mathbf{Y}^k. \\ \mathbf{f}[] : \Theta^n \times \mathbf{U}^m \rightarrow \Theta^n \\ \mathbf{c}[] : \Theta^n \rightarrow \mathbf{Y}^k \end{cases} \quad (1)$$

Here, $\mathbf{x}(t)$ denotes the state variables of the consecutive system; $\dot{\mathbf{x}}(t)$ is its differential variable. $\mathbf{f}[]$ denotes their dynamic model function. $\mathbf{y}(t)$ denotes the observation variables or the variables which are concerned. $\mathbf{c}[]$ denotes their function. In a physical dynamic system, all of the elements in the final reachable set are sometimes

not intuitive or concerned. However, its partial elements are concerned. Therefore, a relevant elements' equation $\mathbf{y}(t) = \mathbf{c}[t, \mathbf{x}(t)]$ is built, which can be used for calculating the final concerned parameters' set $\mathbf{Y}^k \subseteq \mathbf{R}^n$. If there are some inequality or equality constraints in the control process as Eq. (2), then \mathbf{Y}^k will become small, dimensionless, even an empty set $\mathbf{Y}^k \rightarrow \Phi$.

$$\begin{cases} \mathbf{g}[t, \mathbf{x}(t), \mathbf{u}(t)] \leq \mathbf{0} \\ \boldsymbol{\zeta}[t, \mathbf{x}(t)] = \mathbf{0} \end{cases} \quad (2)$$

Here, $\mathbf{g}[]$ and $\boldsymbol{\zeta}[]$ denote the inequality or equality constraints. To review the approaches of computing the orbital reachable set, the previous literatures mainly focused on the following aspects, such as the spacecraft formation flight (Lee and Hwang 2018), collision probability calculation (Bai et al. 2012), geostationary satellites collocation (Li 2014), engagement analysis of exo-atmospheric interceptor (Chai et al. 2014), Earth re-entry (Lu and Xue 2010), and Moon and Mars entry landing footprints (Arslantas 2016; Benito and Mease 2012). Methods vary in different cases, but all of them could be categorized essentially into two types.

Type I:

When a spacecraft is dominated by one force and the orbital state transition matrix can be derived by the linearization hypothesis in some form as $\dot{\mathbf{x}} = \mathbf{A}\mathbf{x} + \mathbf{B}\mathbf{u}$, and if there is no control force or uncertain process model error in the duration $t \in [t_0, t_f]$, a state transition matrix $\Phi_{(t_0, t_f)} = e^{\mathbf{A}(t_f - t_0)}$ can be utilized to compute the final state $\mathbf{x}_{t_f} = \Phi_{(t_0, t_f)}\mathbf{x}_{t_0}$. Therefore, the final state reachable set, affected by an initial state uncertainty or a small orbital maneuver (Zhang et al. 2013; Wen et al. 2018; Yang et al. 2019), can be approximately calculated by the state transition matrix (i.e., $\delta\mathbf{x}_{t_f} = \Phi_{(t_0, t_f)}\delta\mathbf{x}_{t_0}$). If there are cases such as some perturbation forces action on the spacecraft (Li et al. 2011), large uncertainty range of the initial state, long initial-final duration (He et al. 2013), or a complex flight process (Feng et al. 2019), the calculation of the reachable set by the utilization of linearization hypothesis leads to an inaccuracy, or even a wrong result.

Type II:

When a spacecraft has some orbital control powers or there are some uncertain processes, such as the general entry or re-entry reachable set problems with uncertain atmospheric model parameters, the final state becomes more complex as $\mathbf{x}_{t_f} = \Phi_{(t_0, t_f)}\mathbf{x}_{t_0} + \int_{t_0}^{t_f} \mathbf{B}\mathbf{u} \cdot dt$. Because of the unknowable controlling or uncertain perturbation forces $\int_{t_0}^{t_f} \mathbf{B}\mathbf{u} \cdot dt$ during the process, the reachable set cannot be computed by the state transition matrix approach. Komendera et al. (2012) had suggested an intelligent feedback-adjust idea to search the initial parameters

of a reachable set's envelope, but it also needs more computations and is not practical for the complex engineering problems. The practical approach is the two-step method which avoids a huge amount of calculations. Take the Earth re-entry for example (Lu and Xue 2010). The first step computes the maximum range, and the second step computes the maximum cross-ranges with some fixed-ranges which are between the minimum and maximum ranges. The high-precision dynamical model is adopted instead of a linearization assumption. By this way, the reachable set calculated by the high-precision method is undoubtedly more accurate than that calculated by the linearization hypothesis. This method is a calculation strategy operated at two levels. The outer layer gradually gives the virtual objective point, while the inner layer is a general single-objective non-linear constrained optimization problem. According to the specific conditions, the inner optimization problem can be solved by an indirect method or a direct optimization algorithm. The basic model is shown in Eq. (3).

$$\text{Outer} \left\{ \begin{array}{l} \text{search } (J = J_1, J_2, \dots, J_m) \\ \text{Inner} \left\{ \begin{array}{l} \mathbf{x} = [x_1, x_2, \dots, x_n]^T \\ \text{s.t.} \left\{ \begin{array}{l} g_j[\mathbf{x}] \leq 0, j = 1, \dots, l \\ h_k[\mathbf{x}] = 0, k = 1, \dots, p \end{array} \right. \\ [f, g_j, h_k] \in \mathbf{R}^n \\ \min J = f(\mathbf{x}) \end{array} \right. \\ \text{end} \end{array} \right. \quad (3)$$

Here, n, m, l, p denote the number of the optimization variables, optimization objectives, inequality constraints, and equality constraints, respectively. f, g_j, h_k denote the objective function, inequality constraint function, and equality constraint function, respectively. The s.t. is the abbreviations for the subjected to some constraints. The optimization results of the inner layer calculation constitute the envelope parameters of the reachable set. As for

$$\Theta_{t_0}^n = \left\{ \begin{array}{l} \mathbf{x}(t_0) \in \mathbf{R}^n \\ \text{s.t. } \kappa_{EJ2} = (h_{LEO} + R_E), f_{EJ2} = 0, \forall e_{EJ2} < 1, \forall i_{EJ2} \in [i_{EJ2}^{lb}, i_{EJ2}^{ub}] \end{array} \right\}. \quad (4)$$

the shortcoming of this methodology, it is impossible to prove whether the reachable set is continuous or not.

The structure of the remainder of the article is as follows. After reviewing the above-mentioned trans-lunar orbital dynamical models and different approaches of the orbital reachable set generation, details of problem formulation including the generation strategy

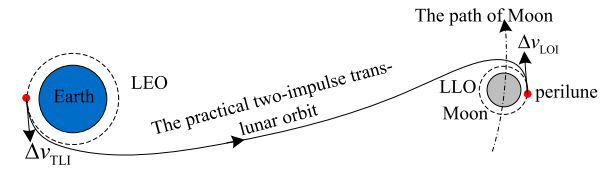


Fig. 1 Illustration of the practical two-impulse trans-lunar orbit

proposed in this paper are presented in “[Problem statement and strategy](#)” section. The retrograde semi-analytical model and the multiple-layer traversal searching approach are described in “[Reachable set rapid generation](#)” section. In “[Precision envelopes generation](#)” section, the retrograde semi-analytical model and the envelope of the reachable set are re-checked by the high-precision dynamics model. The property of the reachable set changes due to some influence factors are exhibited in “[reachable set property measurement](#)” section. Finally, conclusions are drawn in “[Conclusion](#)” section.

Problem statement and strategy

Problem statement

The practical two-impulse trans-lunar orbit has duration about 4~5 days, projected orbital altitudes at the epochs of TLI and LOI, and tangential incremental velocities of Δv_{TLI} and Δv_{LOI} as shown in Fig. 1.

Tangential impulses are reasonable for computing a trans-lunar orbit. It is uneconomical that the trans-lunar burn from a low earth orbit (LEO) with a non-tangential thruster vector. It is same uneconomical for lunar orbit insertion with a non-tangential thruster vector. The TLI burn duration of Apollo-11 is 320 s, it is an impulse compared to the trans-lunar duration about 4–5 days (Berry 1970). To describe the orbital reachable set of the practical two-impulse trans-lunar orbit via the mathematical formula in Eq. (1), t_0 and t_f represent the epochs of TLI and LOI, respectively. The orbital initial state set is described as Eq. (4).

Here, κ represents the radius of periapsis; subscript ‘EJ2’ represents the J2000.0 earth-centric coordinate system; h_{LEO} represents the altitude of LEO; R_E represents the radius of Earth; e, i , and f represent the eccentricity, inclination, and the true anomaly of the trans-lunar orbit, respectively. The superscript of ‘lb’ and ‘ub’ represent the low and upper boundaries. The expression of $e_{EJ2} < 1$

implies the trans-lunar orbit is an elliptical orbit, which orbital energy is lower than the parabolic and hyperbolic orbits. The interval of $[i_{EJ2}^{lb}, i_{EJ2}^{ub}]$ depends on the launching angle A_0 and the latitude of launch of launch site of B_0 , i.e., $\cos i_E = \sin A_0 \cos B_0$. The equation of $f_{EJ2} = 0$ is equivalent to that Δv_{TLI} is tangential.

The nominal orbit does not need any mid-course corrections. The reachable set of the orbital elements at t_f can be described as Eq. (5).

$$\Omega_{t_f}^n = \left\{ \begin{array}{l} \mathbf{x}(t_f) \in \mathbf{R}^n \\ \exists t_f > t_0 \\ \text{s.t. } \kappa_{MJ2} = (h_{LLO} + R_M), f_{MJ2} = 0, \forall e_{MJ2} > 1, \forall \Delta t = (t_f - t_0) \in [\Delta t^{lb}, \Delta t^{ub}] \end{array} \right\}. \quad (5)$$

Here, the subscript of 'MJ2' represents the J2000.0 moon-centric coordinate system; h_{LLO} represents the altitude of LLO; and R_M represents the radius of Moon. The expression of $e_{MJ2} > 1$ implies that the trans-lunar orbit is a hyperbolic orbit when it arrives at the perilune point. The equation of $f_{MJ2} = 0$ is equivalent to that Δv_{LOI} acts on the perilune point. The interval of $[\Delta t^{lb}, \Delta t^{ub}]$ implies that the acceptable trans-lunar duration is practical and useful in an engineering task.

Obviously, the reachable set as described in Eq. (5) is a multi-dimensional element set, which is difficult to present clearly and simply understand. However, only the inclination and the longitude of ascending node (LAN) in the lunar centric-fixed coordinate system (i.e., the

subscript of 'LCF') in Eq. (6) are the elements concerned, which affect the ground track of satellite (GTS) after lunar orbit insertion as shown in Fig. 2.

$$\mathbf{Y}_{t_f}^k = \left\{ (i_{LCF}, \Omega_{LCF}) : \forall \mathbf{x}(t_f) \in \Omega_{t_f}^n \right\}. \quad (6)$$

Two-step strategy

It implies that there are countless trans-lunar orbits with constraints as Eq. (7) to be calculated for generating a valid $\mathbf{Y}_{t_f}^k$. The difficulty lies in two aspects, one is the orbital dynamics model and another is the optimization algorithm. If the high-precision orbital mode is applied, its computing-time for a large number of the orbits is unaffordable. And if the evolutionary algorithm is applied, it leads to the same problem of the cost of computing.

Reference *Type II*, mentioned in the bottom of the Introduction, a strategy is suggested, which contains two steps as shown in Fig. 3. The simple explanation is as follows:

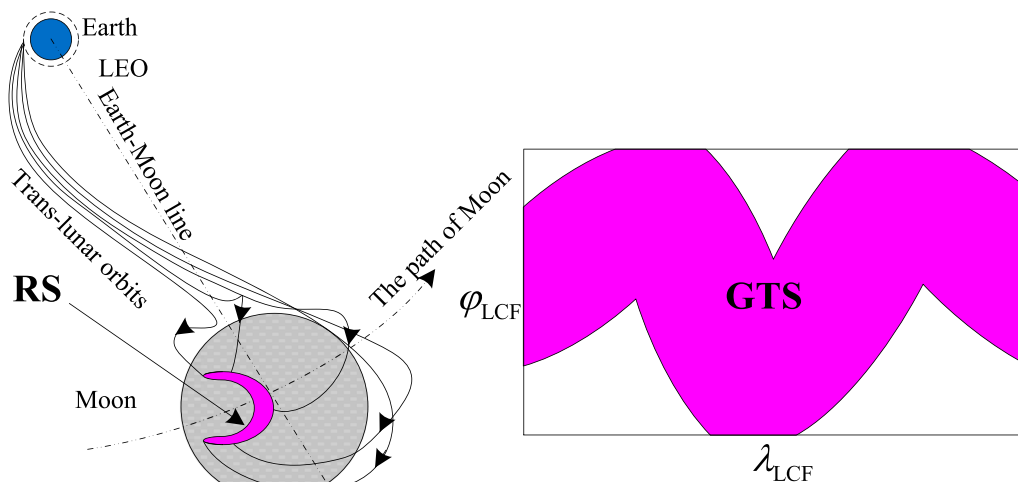


Fig. 2 Illustration of the reachable set and the GTS of the trans-lunar orbits

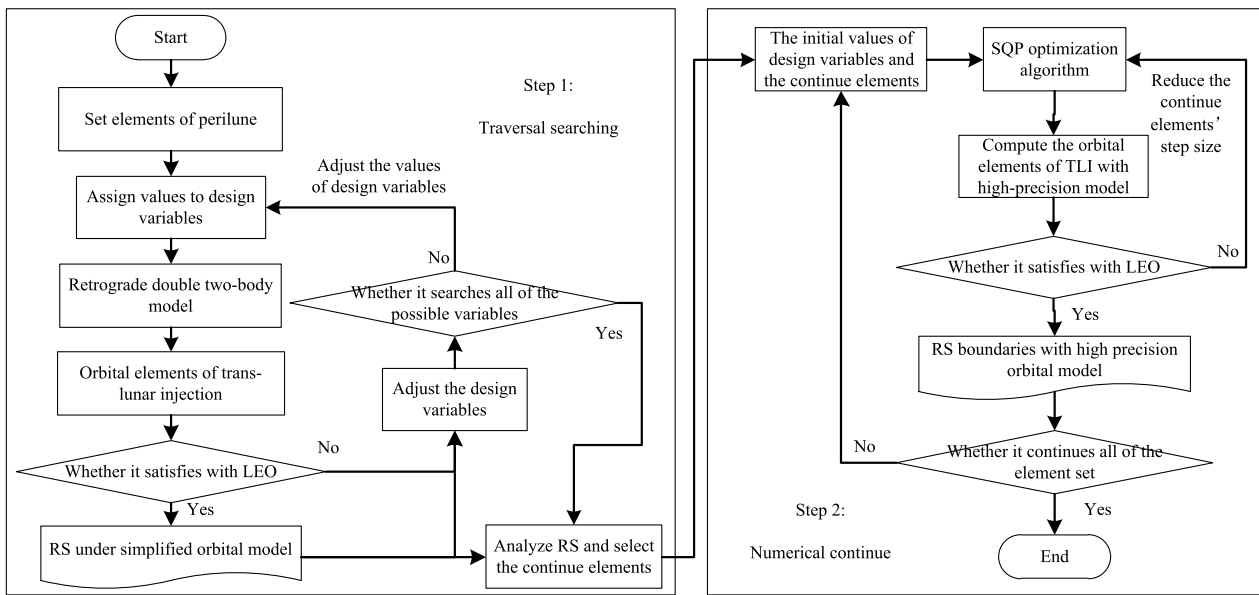


Fig. 3 Flow chart of the frame suggested for generating the reachable set of the trans-lunar orbits

$$\begin{cases} \mathbf{x} = \mathbf{x}(t_0) \\ \text{s.t.} \begin{cases} \kappa_{EJ2} = (h_{LEO} + R_E), e_{EJ2} < 1, i_{EJ2} \in [i_{EJ2}^{lb}, i_{EJ2}^{ub}], f_{EJ2} = 0 \\ \kappa_{MJ2} = (h_{LLO} + R_M), e_{MJ2} > 1, f_{MJ2} = 0, \Delta t = (t_f - t_0) \in [\Delta t^{lb}, \Delta t^{ub}] \end{cases} \end{cases}. \quad (7)$$

Step 1:

A retrograde semi-analytical model is established based on the double two-body concept, wherein the orbital elements at the perilune point are selected to play the role of the traversal searching variables. After traversal searching, the orbital elements, which satisfy the constraints, are recorded. Then, the topological structure and the influence relations of the elements in the reachable set are analyzed.

Step 2:

The orbital design variable, which affects the reachable set obviously, is selected to play the role of the numerical continuation element. Then, the precision envelopes of the reachable set are re-checked with the high-precision orbital dynamical model under the continuation frame. Every point of the envelope implies a constrained optimal problem. Its solution is solved via the initial values from Step 1 via SQP optimization algorithm (Gill et al. 2005).

Step 1 not only provides the topological structure information and the influence relation of the design variables in the reachable set but also provides the initial value of the orbit design variables for Step 2. Step 2 checks the

reachable set solved by Step 1 using the proven high-precision orbital dynamical model.

Reachable set rapid generation

A retrograde semi-analytical model

The latitude and longitude on the Moon's influence sphere, and flight duration from TLI to the moment when the lunar probe passes into the Moon's influence sphere are selected as the trans-lunar orbital design

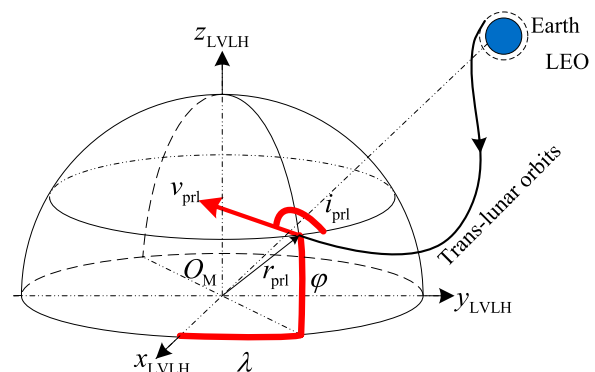


Fig. 4 Illustration of the orbital design variables at the moment of perilune

variables (Peng et al. 2011; Gao et al. 2018). The Newton iteration is applied to calculate the Earth-centered true of anomaly of the entrance point on the Moon's influence sphere, and then the trans-lunar orbit before the moment when the lunar probe passes into the Moon's influence sphere can be designed. The orbital design variables in the traditional application of the double two-body model cannot obtain a constant orbital altitude at the epoch of perilune point, and the design variables have no physical significance. Moreover, they are not easily translated into the reachable set elements in Eq. (6). In our previous work, a set of orbital elements at the epoch of the perilune suggested as the design variable show a well convergence performance to design the adaptive LEO-phase and the fixed-thrust circumlunar free-return orbits (He et al. 2019). The latitude and longitude (λ, φ) in the lunar-centric local vertical and local horizontal coordinate system (LVLH) at the epoch of perilune, the velocity vector azimuth angle i_{prl} , and the value of the velocity v_{prl} before LOI are selected as the trans-lunar orbital design variables as shown in Fig. 4.

The subscript of 'prl' represents the epoch of the perilune. The trans-lunar orbital position and velocity vectors at this epoch before LOI can be described as Eq. (8).

$$\begin{cases} \mathbf{r}_{\text{prl}}^{\text{LVLH}} = r_{\text{prl}} [\cos \varphi \cos \lambda \quad \cos \varphi \sin \lambda \quad \sin \varphi]^T \\ \mathbf{v}_{\text{prl}}^{\text{LVLH}} = \mathbf{M}_z(-\lambda) \mathbf{M}_y(\varphi) \cdot v_{\text{prl}} [0 \quad \cos i_{\text{prl}} \quad \sin i_{\text{prl}}]^T \end{cases} \quad (8)$$

Here, r_{prl} is equals to κ_{MJ2} ; $\mathbf{M}_y, \mathbf{M}_z$, and unused \mathbf{M}_x are the basic rotation matrix of the coordinate systems. If t_f (i.e., the epoch of LOI) and r_{prl} (i.e., $r_{\text{prl}} = R_M + h_{\text{LLO}}$) are set to constants, the instantaneous lunar-centered LVLH coordinate system can be treated as an inertial system, the position, and velocity vectors of the trans-lunar orbit at this epoch before LOI in J2000.0 moon-centered coordinate system can be computed by Eq. (9).

$$\begin{cases} \mathbf{r}_{\text{prl}}^{\text{MJ2}} = \mathbf{M}_{\text{LVLH2MJ2}} \cdot \mathbf{r}_{\text{prl}}^{\text{LVLH}} \\ \mathbf{v}_{\text{prl}}^{\text{MJ2}} = \mathbf{M}_{\text{LVLH2MJ2}} \cdot \mathbf{v}_{\text{prl}}^{\text{LVLH}} \end{cases} \quad (9)$$

Here, $\mathbf{M}_{\text{LVLH2MJ2}}$ is the rotation matrix from the lunar-centered LVLH coordinate system to the J2000.0 lunar-centered coordinate system which is expressed of $\mathbf{M}_{\text{LVLH2MJ2}} = \mathbf{M}_z(-\Omega_M) \mathbf{M}_x(-i_M) \mathbf{M}_z(-u_M)$. The expressions of (u_M, i_M, Ω_M) are the Moon's argument of latitude, inclination, and right ascension of ascending node (RAAN), respectively, in the J2000.0 lunar-centered coordinate system. Therefore, the trans-lunar orbit can be only computed by ($\lambda, \varphi, i_{\text{prl}}, v_{\text{prl}}$). When $[\mathbf{r}_{\text{prl}}^{\text{MJ2}}, \mathbf{v}_{\text{prl}}^{\text{MJ2}}]$ is translated into the modified classical orbital elements

$(\kappa_{\text{MJ2}}, e_{\text{MJ2}}, i_{\text{MJ2}}, \Omega_{\text{MJ2}}, \omega_{\text{MJ2}}, f_{\text{MJ2}}^{\text{prl}})$, the radius of the Laplace influence sphere ρ is 66200 km. Hence, the true anomaly $f_{\text{in}}^{\text{MJ2}}$ at the moment of t_{in} can be computed by Eq. (10).

$$f_{\text{in}}^{\text{MJ2}} = -\arccos \left[\frac{p_{\text{prl}}}{e_{\text{prl}} \cdot \rho} - \frac{1}{e_{\text{prl}}} \right]. \quad (10)$$

Here, the subscript of 'in' represents the epoch when the lunar module enters the Laplace influence sphere, and $p_{\text{prl}} = \kappa_{\text{prl}}(1 + e_{\text{prl}})$. Then, the position and velocity vectors of the trans-lunar orbit $[\mathbf{r}_{\text{in}}^{\text{MJ2}}, \mathbf{v}_{\text{in}}^{\text{MJ2}}]$ at this epoch in J2000.0 lunar-centered coordinate system can be computed by the principle of the two-body orbital state transfer matrix described as Eq. (11).

$$\begin{bmatrix} \mathbf{r}_{\text{in}}^{\text{MJ2}} \\ \mathbf{v}_{\text{in}}^{\text{MJ2}} \end{bmatrix} = \begin{bmatrix} F & G \\ F_t & G_t \end{bmatrix} \begin{bmatrix} \mathbf{r}_{\text{prl}}^{\text{MJ2}} \\ \mathbf{v}_{\text{prl}}^{\text{MJ2}} \end{bmatrix}, \quad (11)$$

$$\begin{cases} F = 1 - \frac{\rho}{p_{\text{prl}}} (1 - \cos(f_{\text{in}}^{\text{MJ2}})) \\ G = \frac{\rho \cdot r_{\text{prl}}^{\text{MJ2}}}{\sqrt{\mu_M p_{\text{prl}}}} \sin(f_{\text{in}}^{\text{MJ2}}) \\ F_t = \frac{\sqrt{\mu_M}}{r_{\text{prl}}^{\text{MJ2}} \cdot p_{\text{prl}}} [\sigma_{\text{prl}}^{\text{MJ2}} \cdot (1 - \cos(f_{\text{in}}^{\text{MJ2}})) - \sqrt{p_{\text{prl}}} \sin(f_{\text{in}}^{\text{MJ2}})] \\ G_t = 1 - \frac{r_{\text{prl}}^{\text{MJ2}}}{p_{\text{prl}}} (1 - \cos(f_{\text{in}}^{\text{MJ2}})) \end{cases} \quad (12)$$

Here, μ_M represents the lunar gravitational constant, and $\sigma_{\text{prl}}^{\text{MJ2}} = (\mathbf{r}_{\text{prl}}^{\text{MJ2}} \cdot \mathbf{v}_{\text{prl}}^{\text{MJ2}}) / \sqrt{u_M}$.

According to Gudermann Christoph's transformation principle, the lunar-centered hyperbolic anomaly H at this epoch can be computed by Eq. (13).

$$\begin{cases} \cosh H = (e_{\text{prl}} + \cos f_{\text{in}}^{\text{MJ2}}) / (1 + e_{\text{prl}} \cos f_{\text{in}}^{\text{MJ2}}) \\ \sinh H = (\sqrt{e_{\text{prl}}^2 - 1} \sin f_{\text{in}}^{\text{MJ2}}) / (1 + e_{\text{prl}} \cos f_{\text{in}}^{\text{MJ2}}) \\ H = \ln(\cosh H + \sinh H) \end{cases} \quad (13)$$

The flight duration from t_{in} to t_f can be computed by Eq. (14).

$$\Delta t_{\text{in2prl}} = \sqrt{-\frac{1}{\mu_M} \left(\frac{\kappa_{\text{prl}}}{1 - e_{\text{prl}}} \right)^3} \cdot (e_{\text{prl}} \sinh H - H). \quad (14)$$

Therefore, $t_{\text{in}} = t_{\text{prl}} - \Delta t_{\text{in2prl}}$. The Moon's position and velocity vectors $[\mathbf{r}_M^{\text{in}}, \mathbf{v}_M^{\text{in}}]$ are obtained by the JPL ephemeris table. The position and velocity vectors of the trans-lunar orbit $[\mathbf{r}_{\text{in}}^{\text{MJ2}}, \mathbf{v}_{\text{in}}^{\text{MJ2}}]$ at the epoch of t_{in} in J2000.0

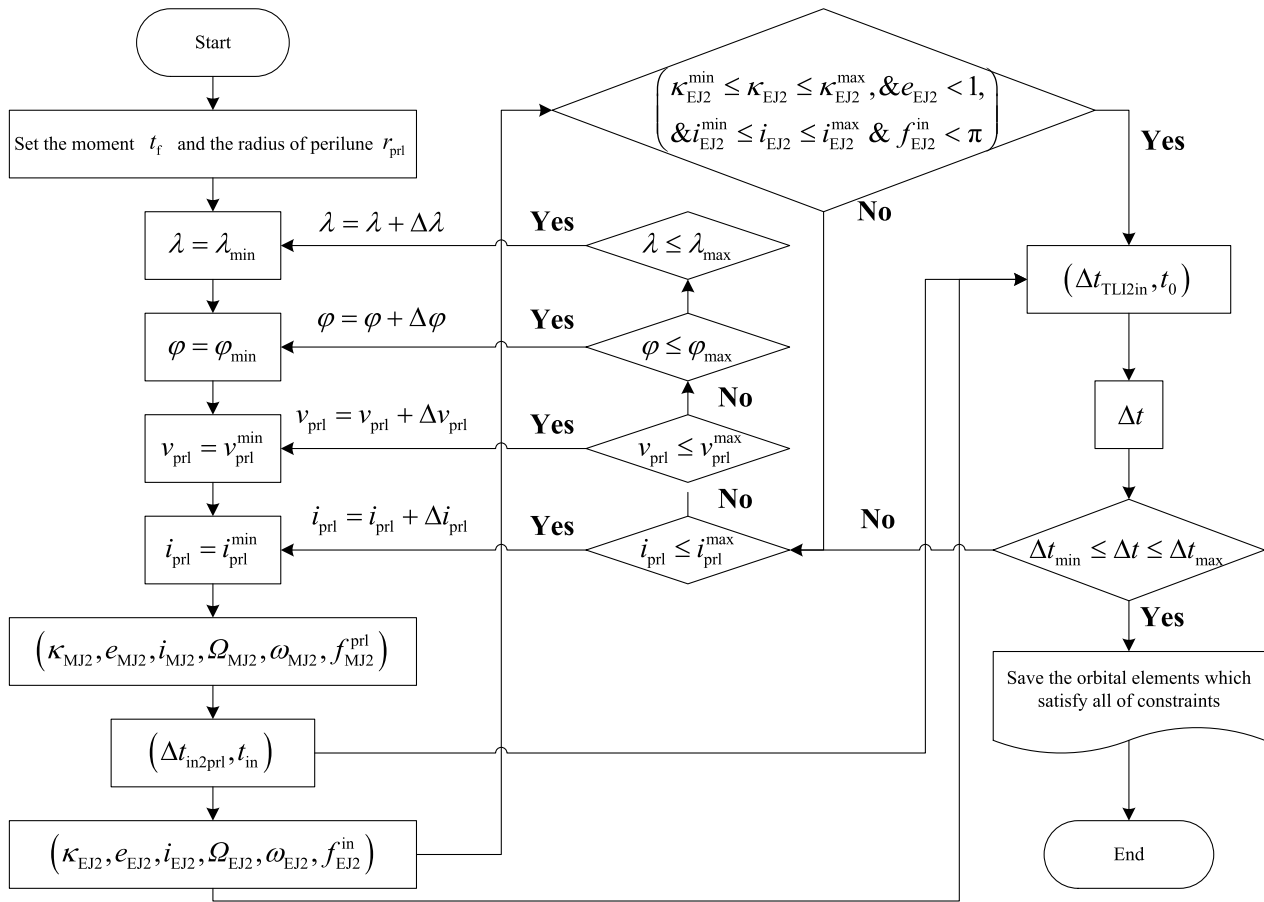


Fig. 5 Flow chart of the multiple-layer traversal search method

Earth-centered coordinate system can be computed by Eq. (15).

$$\begin{cases} \mathbf{r}_{\text{in}}^{\text{EJ2}} = \mathbf{r}_{\text{M}}^{\text{in}} + \mathbf{r}_{\text{in}}^{\text{MJ2}} \\ \mathbf{v}_{\text{in}}^{\text{EJ2}} = \mathbf{v}_{\text{M}}^{\text{in}} + \mathbf{v}_{\text{in}}^{\text{MJ2}} \end{cases} \quad (15)$$

When $[\mathbf{r}_{\text{in}}^{\text{EJ2}}, \mathbf{v}_{\text{in}}^{\text{EJ2}}]$ is translated into the modified classical orbital elements $(\kappa_{\text{EJ2}}, e_{\text{EJ2}}, i_{\text{EJ2}}, \Omega_{\text{EJ2}}, \omega_{\text{EJ2}}, f_{\text{EJ2}}^{\text{in}})$, the eccentricity of e_{EJ2} is smaller than 1, and $f_{\text{EJ2}}^{\text{in}}$ is the true anomaly of the trans-lunar orbit at the epoch of t_{in} . According to the Kepler's transformation principle, the flight duration from the moment of TLI to the moment t_{in} can be computed by Eq. (16).

$$\Delta t_{\text{TLI2in}} = \sqrt{\frac{1}{\mu_{\text{E}}}} \left(\frac{\kappa_{\text{EJ2}}}{1 - e_{\text{EJ2}}} \right)^3 \left(E_{\text{EJ2}}^{\text{in}} - e_{\text{EJ2}} \cdot \sin E_{\text{EJ2}}^{\text{in}} \right). \quad (16)$$

Here, $\tan \frac{E_{\text{EJ2}}^{\text{in}}}{2} = \sqrt{\frac{1 - e_{\text{EJ2}}}{1 + e_{\text{EJ2}}}} \tan \frac{f_{\text{EJ2}}^{\text{in}}}{2}$, and the epoch of TLI (i.e., t_0) is $t_0 = t_{\text{in}} - \Delta t_{\text{TLI2in}}$. The total flight duration of the trans-lunar orbit is $\Delta t = (t_{\text{f}} - t_0) = \Delta t_{\text{TLI2in}} + \Delta t_{\text{in2prl}}$.

The expressions in Eqs. (8, 9, 10, 11, 12, 13, 14, 15, 16) are the so-called retrograde semi-analytical model, which is proposed to compute the trans-lunar orbit rapidly.

Multiple-layer traversal search

Based on the retrograde semi-analytical model, a multi-layer traversal search method is utilized to generate the reachable set of the trans-lunar orbits rapidly. The flow chart is shown in Fig. 5.

$(\lambda, \phi, i_{\text{prl}}, v_{\text{prl}})$ are selected as the traversal searching elements in a four-layer frame respectively. Then, κ_{EJ2} , e_{EJ2} , i_{EJ2} , and, $f_{\text{EJ2}}^{\text{in}}$ are tested by the constraints. If any constraint is not satisfied, the next loop will be re-started. Considering the error of the double two-body model, an error of the radius of perigee $\Delta \kappa_{\text{EJ2}}$ is allowable as Eq. (17).

$$\begin{cases} \kappa_{\text{EJ2}}^{\text{min}} = (h_{\text{LEO}} + R_{\text{E}}) - \Delta \kappa_{\text{EJ2}} \\ \kappa_{\text{EJ2}}^{\text{max}} = (h_{\text{LEO}} + R_{\text{E}}) + \Delta \kappa_{\text{EJ2}} \end{cases} \quad (17)$$

$(\lambda, \phi, i_{\text{prl}}, v_{\text{prl}})$ refresh its values by add themselves on $(\Delta \lambda, \Delta \phi, \Delta i_{\text{prl}}, \Delta v_{\text{prl}})$ in everyone's layer, respectively.

Until the searching process of the four layers is accomplished, the set of the orbital elements at the epoch of perilune constitutes the reachable set.

The reachable set based on the retrograde semi-analytical model

To verify the effectiveness of the proposed retrograde semi-analytical model and the multi-layer traversal search frame, an example is tested. The useful orbital elements and constraints are optioned as follows:

- The moment of perilune t_f is set as 1 Jan 2025 0:00:00.000 UTCG (UTC, in Gregorian Calendar format).
- Refer to Apollo-11 mission (Berry 1970), set $h_{LLO}=111$ km and $h_{LEO}=185.2$ km.
- Set $[\lambda_{\min}, \lambda_{\max}] = [-1, 80, 180]$ deg, $[\varphi_{\min}, \varphi_{\max}] = [-90, 90]$ deg, $\Delta\lambda = \Delta\varphi = 2$ deg. v_{prl} is set to ensure that the trans-lunar orbit is a lunar-centered hyperbolic orbit. Therefore, its minimum value is $v_{prl}^{\min} = \sqrt{2\mu_M / (h_{LLO} + R_M)}$. The allowable $\Delta v_{LOI}^{\text{allow}}$ is smaller than 1 km/s [14]. Its maximum value $v_{prl}^{\max} = \sqrt{\mu_M / (h_{LLO} + R_M) + \Delta v_{LOI}^{\text{allow}}}$. Therefore, $[v_{prl}^{\min}, v_{prl}^{\max}] = [2302.7, 2628.3]$ m/s, and set $\Delta v_{prl} = 1$ m/s. A circumlunar free-return orbit or a hybrid orbit is used to being the trans-lunar orbit of the crew exploration vehicle. Both of them have a retrograde LLO after lunar orbit insertion by a tangential maneuver at perilune. The LLO is destination orbit for the lunar module to rendezvous with the crew exploration vehicle. Therefore, set $[i_{prl}^{\min}, i_{prl}^{\max}] = [90, 270]$ deg, and set $\Delta i_{prl} = 2$ deg.
- According to the large position error of the semi-analytical model, set $\Delta\kappa_{EJ2} = 1000$ km. And to analyze the influence of the flight duration on the reachable set, set $[\Delta t_{\min}, \Delta t_{\max}] = [3, 6]$ day.
- The inclination of the moon's path plane varies between 18 to 28 deg. Considering an orbital inclination error of 2 deg, set $[i_{EJ2}^{\min}, i_{EJ2}^{\max}] = [16, 30]$ deg.

After a pure analytical searching process, a mass of the constrained trans-lunar orbits is obtained. The distributions of the design variables are shown in Fig. 6a, b, c.

The longitude of λ is scattered in $[-100, 0]$ W deg while φ symmetrically is scattered in $[-50, 50]$ deg. The value of the velocity at v_{prl} is scattered in $[2410, 2540]$ m/s. It becomes larger with λ and φ become larger to a certain extent. The inclination of i_{prl} is scattered in $[90-180]$ deg ($\varphi < 0$) and $[180-270]$ deg ($\varphi > 0$), and its value tends to 180 deg from 90 and 270 deg in both directions as λ becomes larger.

The orbital elements concerned as shown in Fig. 6d are the inclination and the LAN in the lunar-centric LVLH and the lunar fixed coordinate systems. The inclination in the lunar-centric LVLH coordinate system is scattered in $[90-180]$ deg. However, when the inclination is less than about 167 deg, the LAN only distributes between about $[80-140]$ deg and $[260-320]$ deg. The case in the lunar fixed coordinate system is similar, except for minor differences caused by the Moon's rotation and libration.

Precision envelopes generation

Optimize a precise trans-lunar orbit

The position and velocity vectors of the trans-lunar orbit at the moment of perilune before LOI in J2000.0 lunar-centered coordinate system $[r_{prl}^{MJ2}, v_{prl}^{MJ2}]$ can be computed by Eq. (8) and (9). Then, the Moon's position and velocity vectors $[r_M^{prl}, v_M^{prl}]$ in the J2000.0 Earth-centered coordinate system at this epoch are computed by JPL ephemeris table. The position and velocity vectors at this epoch in the J2000.0 Earth-centered coordinate system are computed by Eq. (18).

$$\begin{cases} r_{prl}^{EJ2} = r_M^{prl} + r_{prl}^{MJ2} \\ v_{prl}^{EJ2} = v_M^{prl} + v_{prl}^{MJ2} \end{cases} \quad (18)$$

The trans-lunar orbit is computed via a 6-day retrograde-time numerical integration with the initial states of $[r_{prl}^{EJ2}, v_{prl}^{EJ2}]$ using the Runge Kutta 7–8 integrator. The epoch of the perigee is found via the interpolation. Then, the position and velocity are translated into the modified classical orbital elements $(\kappa_{EJ2}, e_{EJ2}, i_{EJ2}, \Omega_{EJ2}, \omega_{EJ2}, f_{EJ2}^{TLI})$. Wherein, $|\sin(f_{EJ2}^{TLI})| < \varepsilon$, which is the determined by the interpolation accuracy. κ_{EJ2} and i_{EJ2} are set as the equality and the inequality constraints due to the rocket. Therefore, the inclination and the RAAN at the epoch of LOI are the same with the target values. The model of searching a precise trans-lunar orbit via an optimal algorithm is shown in Eq. (19).

$$\begin{cases} x = [\lambda, \varphi, v_{prl}, i_{prl}]^T \\ \text{s.t.} \begin{cases} \kappa_{EJ2} - (h_{LEO} + R_E) = 0 \\ i_{EJ2}^{\min} \leq i_{EJ2} \leq i_{EJ2}^{\max} \\ \min J = |i_{MJ2} - i_{MJ2}^{\text{tar}}| + |\Omega_{MJ2} - \Omega_{MJ2}^{\text{tar}}| \end{cases} \end{cases} \quad (19)$$

Here, the superscript 'tar' represents the target values of the orbital elements. To verify the model above, the same constraints and the interval of the design variables are set as that in section (the reachable set based on the retrograde semi-analytical model). The difference is the consideration of the precision perturbation orbital model. It contains the Sun's and the Moon's perturbation,

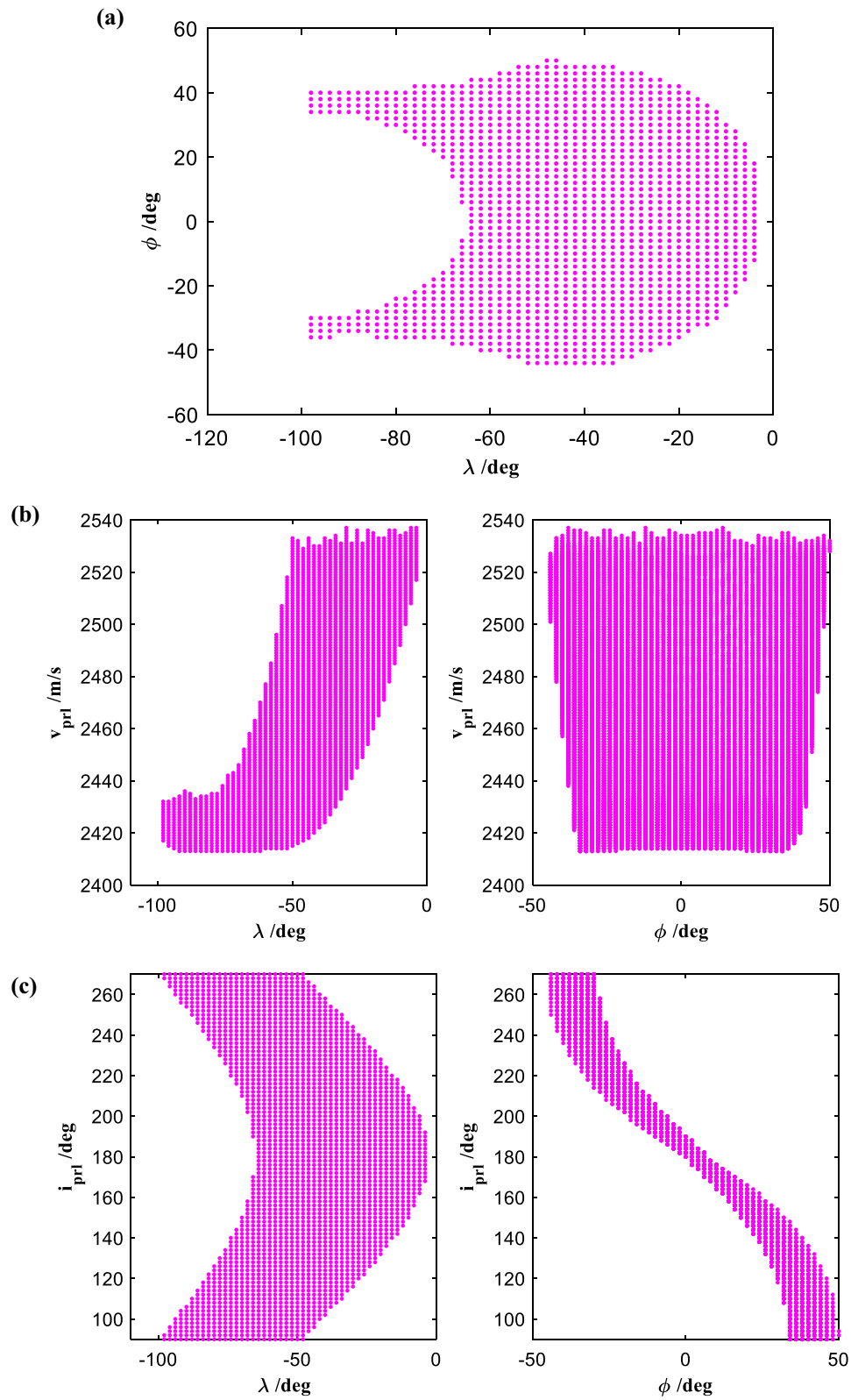


Fig. 6 **a** The distribution of the design variables: λ vs. ϕ . **b** The distribution of the design variables: λ and ϕ vs. v_{prl} . **c** The distribution of the design variables: λ and ϕ vs. i_{prl} . **d** The inclination and LAN in LVLH frame and LCF frame

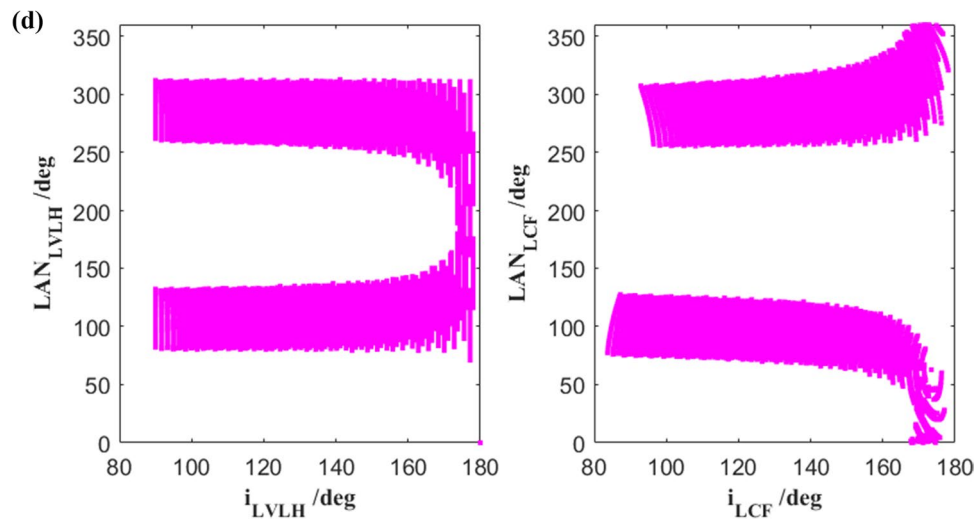


Fig. 6 continued

Table 1 The initial values of the design variables by the retrograde semi-analytical model

Design variables	λ/deg	φ/deg	$v_{\text{pr}}/\text{m/s}$	i_{pr}/deg
Values	-64	-24	2415	228

and the Earth's non-spherical perturbation of 6×6 order of in WGS84 table. The solar radiation pressure and the atmosphere perturbation are ignored. An LLO with $i_{\text{MJ2}}^{\text{tgt}} = 150$ deg and $\Omega_{\text{MJ2}}^{\text{tgt}} = 50$ deg is selected as the destination orbit in an optional manner.

A set of proximate design variables and the lunar-centered modified classical orbital elements in different lunar-centered coordinate systems are listed in Table 1 and Table 2. The Earth-centered modified classical orbital elements at the moment of TLI computed by the retrograde semi-analytical model are listed in Table 3.

Table 4 The optimal values of the design variables with the high-precision model

Design variables	λ/deg	φ/deg	$v_{\text{pr}}/\text{m/s}$	i_{pr}/deg
Values	-64.3936	-24.2613	2456.21	228.1633

The values in Table 1 are selected to play the role of the initial values of the design variables in Eq. (19). The optimal values of the design variables, the lunar-centered modified classical orbital elements in different lunar-centered coordinate systems, and the Earth-centered modified classical orbital elements computed via Eq. (19) with the high-precision numerical integration are listed in Tables 4, 5, and 6, respectively.

The iterative process of the optimal objective function and the constraints' fitness are shown in Fig. 7. The iteration converges quickly within 10 steps. It has two major

Table 2 The lunar-centered modified classical orbital elements by the retrograde semi-analytical model at LOI epoch

Coordinate systems	$\kappa_{\text{MJ2}}/\text{m}$	e_{MJ2}	$i_{\text{MJ2}}/\text{deg}$	Ω/deg	$\omega_{\text{MJ2}}/\text{deg}$	$f_{\text{MJ2}}/\text{deg}$
Lunar-centered LVLH	1,849,200	1.19976	127.6819	95.8856(LAN)	149.0733	0
LCF	1,849,200	1.20592	133.4608	273.8549(LAN)	153.3355	0
J2000 Lunar-centered	1,849,200	1.19976	150.0296	50.8816(RAAN)	176.8663	0

Table 3 The Earth-centered modified classical orbital elements computed by the retrograde semi-analytical model at TLI epoch

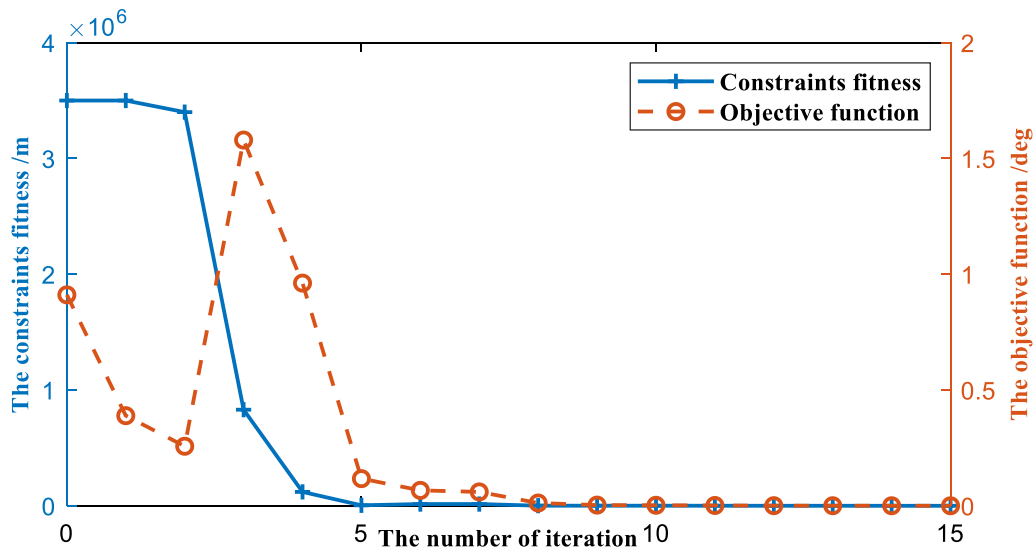
$\kappa_{\text{EJ2}}/\text{m}$	e_{EJ2}	$i_{\text{EJ2}}/\text{deg}$	$\Omega_{\text{EJ2}}/\text{deg}$	$\omega_{\text{EJ2}}/\text{deg}$	$f_{\text{EJ2}}/\text{deg}$	$\Delta t/\text{day}$
7462500	0.96192	25.0860	22.5152	94.6927	0.00000	4.90386

Table 5 The lunar-centered modified classical orbital elements with the high-precision model at LOI epoch

Coordinate systems	κ_{MJ2}/m	e_{MJ2}	i_{MJ2}/deg	Ω/deg	ω_{MJ2}/deg	f_{MJ2}/deg
Lunar-centered LVLH	1849200	1.27547	127.4522	95.4101(LAN)	148.8292	0
LCF	1849200	1.28171	133.2580	273.3152(LAN)	153.0107	0
J2000 Lunar-centered	1849200	1.27547	149.9998	49.9998(RAAN)	176.1479	0

Table 6 The Earth-centered modified classical orbital elements computed with the high-precision model at TLI epoch

κ_{EJ2}/m	e_{EJ2}	i_{EJ2}/deg	Ω_{EJ2}/deg	ω_{EJ2}/deg	f_{EJ2}/deg	$\Delta t/day$
6564074	0.96691	28.5008	61.4684	60.2577	359.7095	5.0708

**Fig. 7** The iterative process of the optimal objective function and the constraints fitness

reasons: One is the utilization of the SQP_snopt optimization kit (Gill et al. 2005), which has good ability to solve non-linear programming problems (Song et al. 2020). Another is the design variables obtained from the retrograde semi-analytical model, which provides an effective initial values.

Re-check the envelope of the reachable set

The reachable set is generated rapidly and clearly based on the retrograde semi-analytical model, and the accuracy of its envelope still has errors. According to the methodology in Eq. (3) and Fig. 6(c), i_{prl} is selected to play the role of the continuation element. In the continuation frame, there are three design variables left. $[i_{EJ2}^{\min}, i_{EJ2}^{\max}]$ is still set as an inequality constraint, and the trans-lunar orbit is numerical integrated via a time-retrograde manner with a fixed Δt . The error absolute

value between the perigee radius and the radius of LEO is set as the optimal objective function. The frame is shown in Eq. (20).

$$\text{Outer} \left\{ \begin{array}{l} \text{search} \left(i_{prl} = i_{prl}^{lb} : i_{prl}^{step} : i_{prl}^{ub} \right) \\ \text{Inner} \left\{ \begin{array}{l} \mathbf{x} = [\lambda, \varphi, v_{prl}]^T \\ \text{s.t.} \left\{ \begin{array}{l} i_{EJ2}^{\min} \leq i_{EJ2} \leq i_{EJ2}^{\max} \\ \min J = |\kappa_{EJ2} - (h_{LEO} + R_E)| \rightarrow 0 \end{array} \right. \end{array} \right. \\ \text{end} \end{array} \right. \quad (20)$$

The initial values \mathbf{x}^0 of the design variables are found from the reachable set in section (the reachable set based on the retrograde semi-analytical model). \mathbf{x}_{n-1}^{opt} plays the role of the initial values for the iteration optimization that $n \geq 2$ as shown in Eq. (21). The orbital

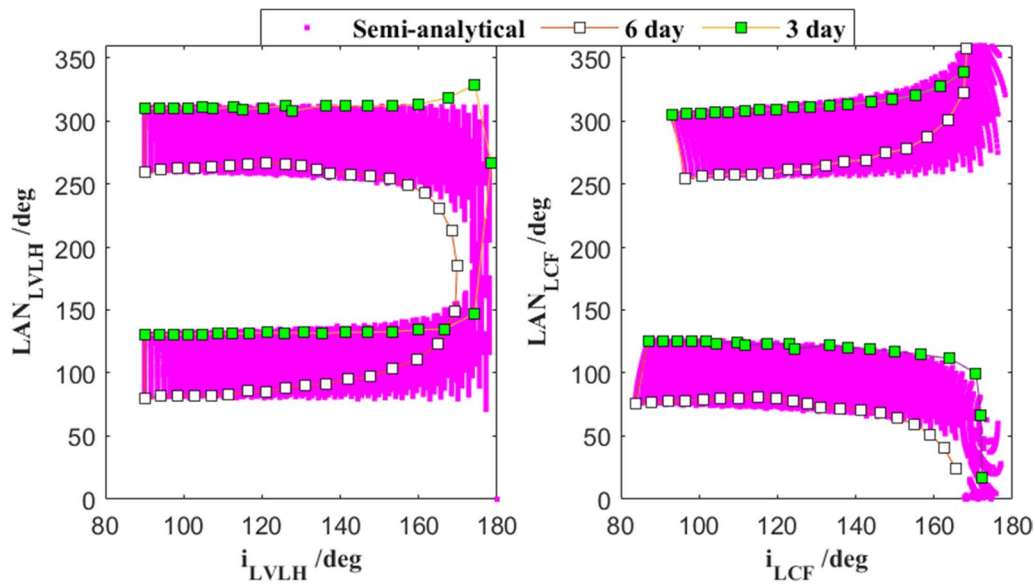


Fig. 8 The envelope of the inclination and LAN in LVLH frame and LCF frame with a 3-day and a 6-day trans-lunar durations

elements are solved quickly and easily using this continuation theory, the envelope of the reachable set are constituted with them.

$n = 0$;

$$\left\{ \begin{array}{l} \text{search } (i_{\text{prl}} = i_{\text{prl}}^{\text{lb}} : i_{\text{prl}}^{\text{step}} : i_{\text{prl}}^{\text{ub}}) \\ \quad n = n + 1; \\ \quad \text{if } n = 1 : \left\{ \begin{array}{l} x_1^{\text{ini}} = x^0 \\ \text{s.t. } \begin{cases} i_{\text{EJ2}}^{\text{min}} \leq i_{\text{EJ2}} \leq i_{\text{EJ2}}^{\text{max}} \\ \min J = |\kappa_{\text{EJ2}} - (h_{\text{LEO}} + R_{\text{E}})| \rightarrow 0 \end{cases} \end{array} \right. \\ \quad \text{elseif } n > 1 : \left\{ \begin{array}{l} x_n^{\text{ini}} = x_{n-1}^{\text{opt}} \\ \text{s.t. } \begin{cases} i_{\text{EJ2}}^{\text{min}} \leq i_{\text{EJ2}} \leq i_{\text{EJ2}}^{\text{max}} \\ \min J = |\kappa_{\text{EJ2}} - (h_{\text{LEO}} + R_{\text{E}})| \rightarrow 0 \end{cases} \end{array} \right. \\ \quad \text{end} \\ \text{end} \end{array} \right. \quad (21)$$

Corresponding to the time-retrograde integrate fixed time $\Delta t \in [3, 6]$ day, respectively, the envelope of the reachable set in the lunar-centered LVLH and the lunar fixed coordinate systems is shown in Fig. 8.

It shows that the model error of the retrograde semi-analytical model for the practical trans-lunar orbit with 6-day duration is larger than that with 3-day flight duration. When the flight duration is 3 days, the

envelope solution of the reachable set is more consistent with the solution computed with the high-precision model. The inclinations in the lunar-centered LVLH and the lunar-centered fixed coordinate systems both approach to 180 deg. When the inclination is close to 180 deg, the LAN has a large error than other cases due to its numerical singularity.

Reachable set property measurement

The property of the reachable set changes due to some influence factors. It is useful to understand the relation of them for designing a manned lunar task in the overall design phase. In consideration of the effectiveness of the retrograde semi-analytical model, the property of the reachable set is measured. The distance of the Earth–Moon, the transfer duration, and the declination of the Moon are tested as follows, respectively.

The distance of the Earth–Moon

The eccentricity of the Moon's path changes from 1/23 to 1/5. It leads a result that the distance of the Earth–Moon changes from about 3.6×10^8 to 4.1×10^8 m in a lunation. After 1 Jan 2025 0:00:00.000 UTCG, 8 Jan 2025 0:00:00.000 UTCG, and 21 Jan 2025 5:00:00.000 UTCG in this lunation are selected as the epochs for testing, which correspond the nearest and the farthest Earth–Moon distances, respectively.

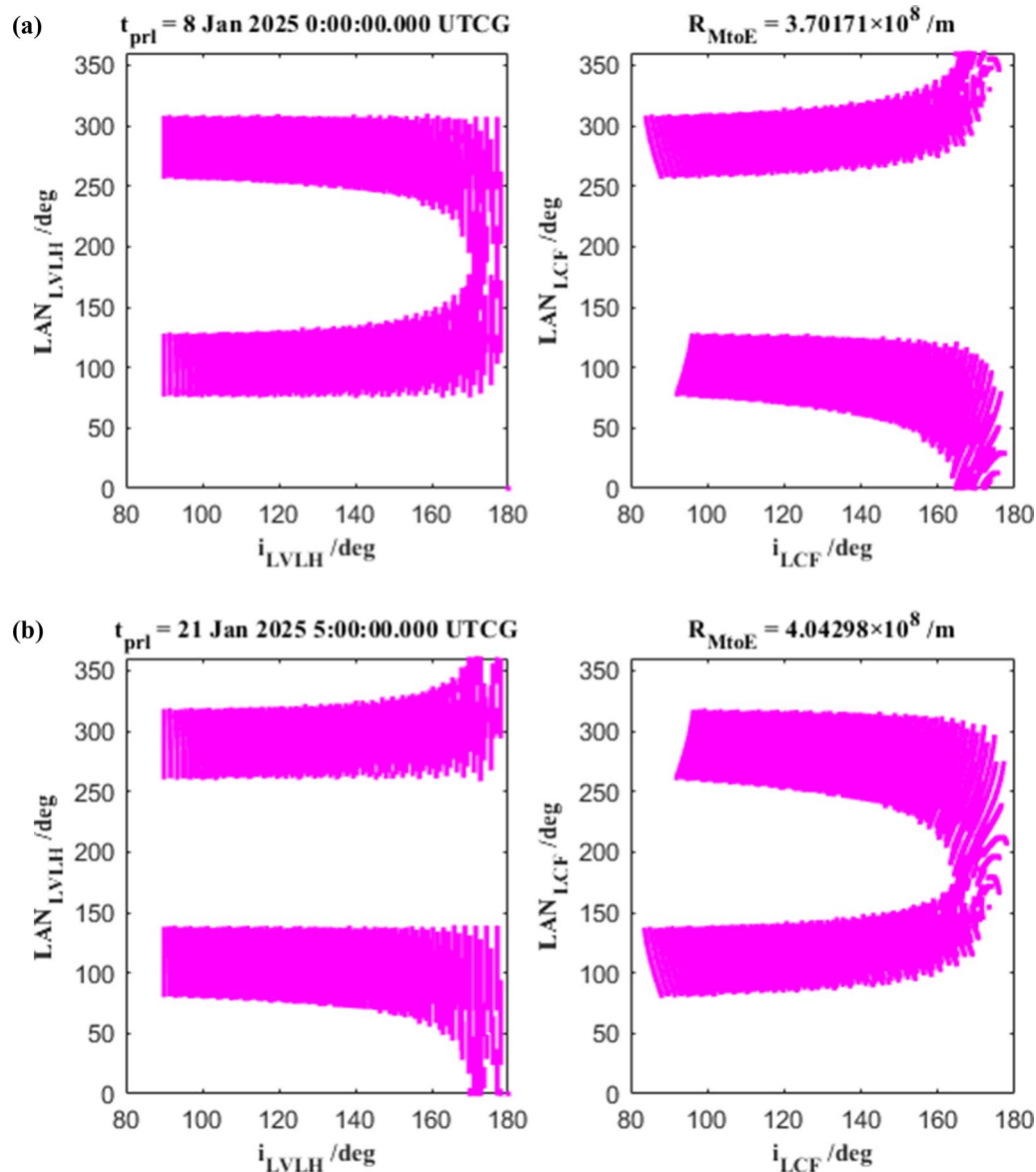


Fig. 9 **a** The inclination and LAN in LVLH frame and LCF frame with the nearest value of the Earth–Moon distance. **b** The inclination and LAN in LVLH frame and LCF frame with the farthest value of the Earth–Moon distance

The results are shown in Fig. 9a, b. It shows outwardly that the Earth–Moon distance leads non-obvious influence to the reachable set except for the orbital inclination is approaching to 180 deg in the lunar-centered LVLH frame. In practice, however, when the orbital inclination is approaching to 180 deg in the lunar-centered LVLH frame, the singularities of LAN emerge. Arbitrary value of LAN does not have significance. In a word, the Earth–Moon distance leads non-obvious influence to the reachable set.

The transfer duration

The reachable sets with the trans-lunar duration of 3 days, 4 days, 5 days, and 6 days are shown in Fig. 10, respectively. All of them arrive at the epoch of 1 Jan 2025 0:00:00.000 UTCG as perilune.

It shows that the LANs in the lunar-centered LVLH and the lunar-centered fixed coordinate systems have distinguishing features. Both of them has two manners (i.e., ascent orbit and descent orbit) arriving their perilune. When the trans-lunar duration is longer than 4 days, the

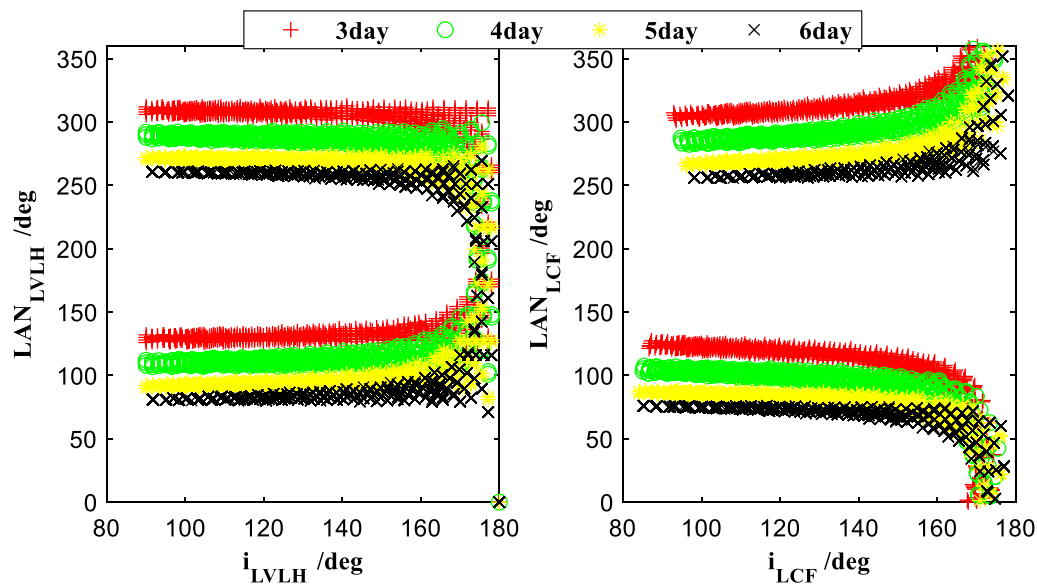


Fig. 10 The inclination and LAN in LVLH frame and LCF frame with different trans-lunar durations

perilune point is on the front of the Moon (i.e., the side is directly visible from the Earth). This property is significant for directly tracking and controlling from the Earth's surface tracking stations.

The declination of the Moon

The Moon's position in the J2000 Earth-centric coordinate system is described via the right ascension and declination. The declination of the Moon describes the Moon's position along the perpendicular direction of the J2000.0 mean equatorial plane. After 1 Jan 2025 0:00:00.000 UTCG, 7 Jan 2025 00:00:00.000 UTCG and 12 Jan 2025 00:00:00.000 UTCG in this lunation are selected as the epochs, which correspond the smallest and the biggest cases of the moon's declinations. The values of the Moon's declinations are 1.359 deg and 28.447 deg, respectively. The reachable sets are shown, respectively, in Fig. 11a, b. Refer to the discussion of the singularities of LAN when the orbital inclination is approaching to 180 deg, when we compare the difference between Fig. 9a, b. The reachable sets have non-obvious difference if just looking at these two pictures. However, the distributions of the LEO inclination as shown in Fig. 12 have a significant difference. It implies that if the inclination of LEO is less than the declination of the Moon, no trans-lunar orbit exists.

In other words, the reachable set is an empty set. The long period of the declination of the Moon is the Metonic cycle (i.e., 18.6 years), which periodically changes from 18.3 to 28.6 deg. The maximum declination of the Moon will be 28.6 deg in 2025 and the minimum is 18.3 deg in 2034. As long as the inclination of LEO is greater than 18.3 deg in 2034, the reachable set of the trans-lunar orbit will not be an empty set. Moreover, the reachable set of the trans-lunar orbit does not become a non-empty set at any time in 2025, and the inclination of the LEO must be greater than 28.6 deg.

Conclusion

A retrograde semi-analytical model is suggested to generate the reachable set of the practical two-impulse trans-lunar orbit with two tangential maneuvers. Compared with the traditional two-body conic method in the literatures, this model does not have internal iteration, and its perilune point altitude can be an accurate constant. The multi-layer traversal searching frame and the precision envelopes re-check have exhibited its rapidity and effectiveness. The classical influence factor test exhibits the changeable property of the reachable set. Some conclusions can be drawn as follows:

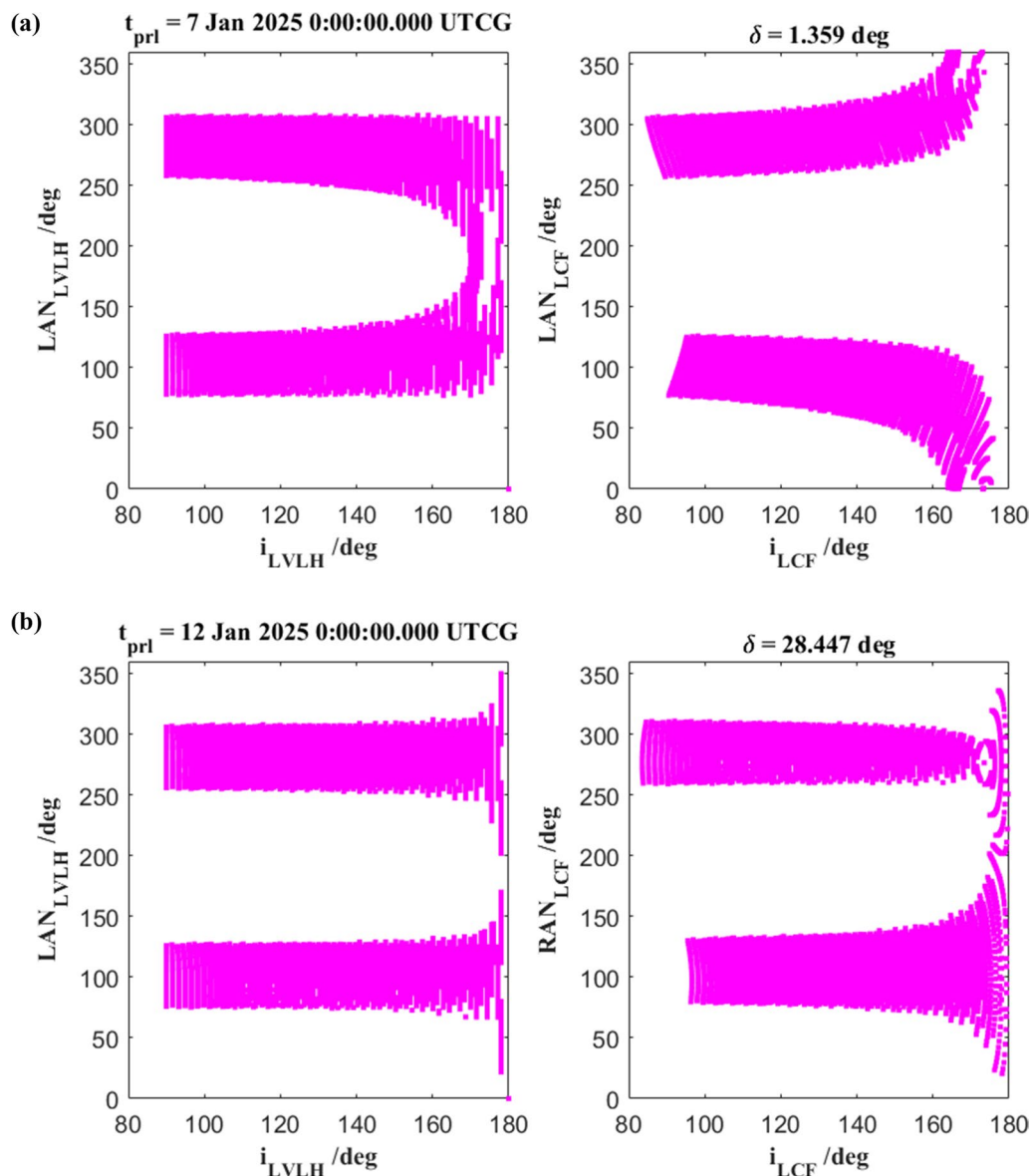


Fig. 11 **a** The inclination and LAN in LVLH frame and LCF frame with the smallest declination of the Moon. **b** The inclination and LAN in LVLH frame and LCF frame when the Moon's declination is the biggest

- A) The distance of the Earth–Moon leads non-obvious influence to the reachable set.
- B) The trans-lunar duration leads to different perilune point on the Moon's surface. If there are only tracking stations on the Earth's surface, and a necessary support of the tracking and control for the lunar

module's LOI, the trans-lunar duration is suggested to be more than 4 days.

- C) It is a necessary condition that the inclination of LEO is greater than the declination of the Moon at the epoch of perilune. Otherwise, the reachable set of the trans-lunar orbits becomes an empty set.

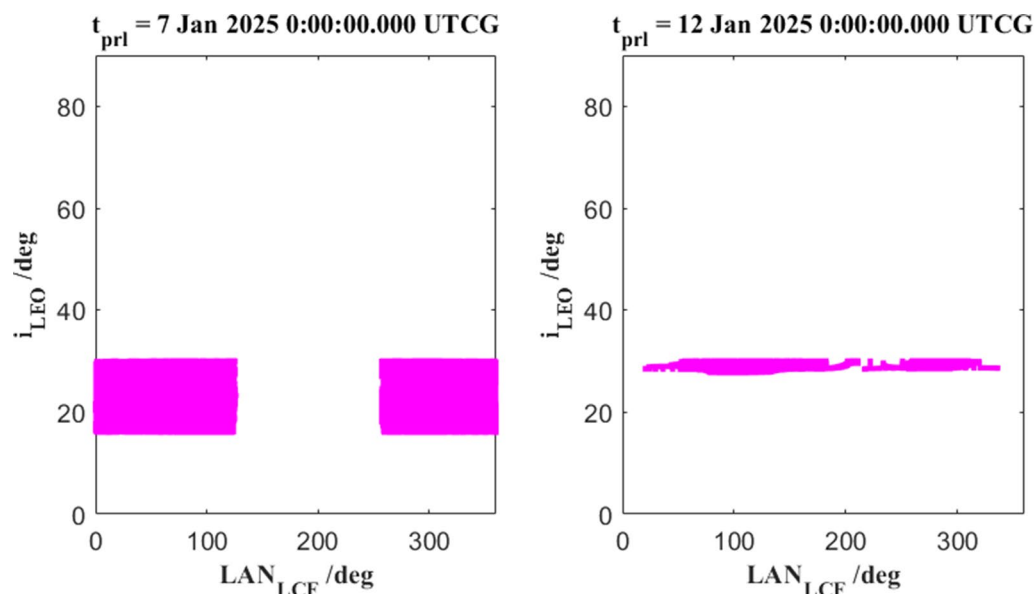


Fig. 12 The LEO inclination distributions when the lunar declination absolute value is the smallest and the biggest

Abbreviations

NASA	National Aeronautics and Space Administration
LLO	Low lunar orbit
LEO	Low earth orbit
TLI	Trans-lunar injection
LOI	Lunar orbit insertion
CR3BP	Circular restricted three-body problem
JPL	Jet Propulsion Laboratory
LAN	Longitude of ascending node
LCF	Lunar centric fixed
GTS	Ground track of satellite
LVLH	Local vertical and local horizontal

Acknowledgements

Not applicable.

Author contributions

The idea of rapidly calculating the reachable set of the lunar module's practical trans-lunar orbit using the lunar perilune elements was put forward by Mr. B-YH. B-YH and S-GW completed the derivation of retrograde semi-analytic model. B-YH completed the coding, figures plotting, and manuscript writing work. Pro. H-NL proofread the manuscript. All the authors read and approved the final manuscript.

Authors' information

Bo-yong He, Associate Prof. received his Ph.D. degree in aeronautical and astronautical science and technology from National University of Defense Technology, China, in 2017. After graduation from doctoral, he joined State Key Laboratory of Astronautic Dynamics (ADL), Xi'an Satellite Control Center as an assistant professor, Xi'an, China in 2018, and in Northwestern Polytechnical University, China, as a postdoctoral fellow (2019–2021). Currently, he implements 1 project from National Natural Science Foundation of China, 1 project from the China Postdoctoral Science Foundation, and 1 project from Young Elite Scientists Sponsorship Program by CAST. His area of expertise is in space mission planning and astrodynamics.

Funding

This work was supported by the National Natural Science Foundation of China (No. 11902362) and the Young Elite Scientists Sponsorship Program by CAST(2021-JCJQ-QT-027).

Availability of data and materials

Not applicable.

Declarations

Competing interests

The authors declare that we have no known competing financial interests or personal relationships that could have appeared to influence the work reported in this paper, and the financial interests/personal relationships, which may be considered as potential competing interests.

Author details

¹State Key Laboratory of Astronautic Dynamics (ADL), Xi'an Satellite Control Center, Xi'an 710043, China.

Received: 29 January 2022 Accepted: 10 February 2023

Published online: 10 March 2023

References

- Arsilantas YE, Oehlschlaegel T, Sagliano M (2016) Safe landing area determination for a moon lander by reachability analysis. *Acta Astronaut* 128(11–12):607–615. <https://doi.org/10.1016/j.actaastro.2016.08.013>
- Bai XZ, Chen L, Tang GJ (2012) Periodicity characterization of orbital prediction error and Poisson series fitting. *Adv Space Res* 50(5):560–575. <https://doi.org/10.1016/j.asr.2012.05.018>
- Benito J, Mease KD (2012) Reachable and controllable sets for planetary entry and landing. *J Guid Control Dyn* 33(3):641–654. <https://doi.org/10.2514/1.47577>
- Berry RL (1970) Launch window and trans-lunar orbit, lunar orbit, and trans-earth orbit planning and control for the Apollo 11 lunar landing mission. AIAA 8th Aerospace Sciences Meeting, New York. No. 70–0024. <https://doi.org/10.2514/6.1970-24>
- Byrnes DV, Hooper HI (1970) Multi-conic: a fast and accurate methods of computing space flight trajectories. AAS/AIAA Astrodynamics conference. Santa Barbara, California. 1970. <https://doi.org/10.2514/6.1970-1062>

- Chai H, Liang YG, Chen L et al (2014) Reachable set modeling and engagement analysis of exo-atmospheric interceptor. *Chin J Aeronaut* 27(6):1513–1526. <https://doi.org/10.1016/j.cja.2014.10.018>
- Colaprete A, Schultz P, Heldmann J (2010) Detection of water in the LCROSS ejecta plume. *Science* 330(6003):463–468. <https://doi.org/10.1126/science.1186986>
- Condon G (2007) Lunar orbit insertion targeting and associated outbound mission design for lunar sortie missions. In: Proceedings of the 2007 AIAA Guidance, Navigation, and Control Conference and Exhibit, Hilton Head, SC, No. 1–27. <https://doi.org/10.2514/6.2007-6680>
- Davis J (2018) Some snark (and details!) about NASA's proposed lunar space station. [EB/OL]. (2018-02-26) [2019-03-24]. <https://www.planetary.org/articles/20180226-lap-g-snark-details>
- Egorov VA (1958) Certain problem of moon flight dynamics. New York, Russian Literature of Satellite, Part I, International Physical Index Inc. p 36–42
- Feng JL, Armellin R, Hou XY (2019) Orbit propagation in irregular and uncertain gravity field using differential algebra. *Acta Astronaut* 161(8):338–347. <https://doi.org/10.1016/j.actaastro.2019.05.045>
- Gao YF, Wang ZK, Zhang YL (2018) Analytical design methods for transfer trajectories between the Earth and the lunar orbital station. *Astrophys Space Sci* 363:206. <https://doi.org/10.1007/s10509-018-3426-7>
- Garn M, Qu M, Chrono J (2008) NASA's planned return to the moon: global access and anytime return requirement implications on the lunar orbit insertion burns. In: Proceedings of the 2008 AIAA/AAS Astrodynamics Specialists Conference, Honolulu, HI, No. 1–20. <https://doi.org/10.2514/6.2008-7508>
- Gill PE, Murray W, Sunder MA (2005) SNOPT: an SQP algorithm for large-scale constrained optimization. *SIAM Rev* 47:99–131. <https://doi.org/10.1137/S0036144504446096>
- Grantham WJ (1981) Estimating reachable sets. *J Dyn Syst Meas Control* 103(4):420–422. <https://doi.org/10.1115/1.3139685>
- He BY, Shen HX (2020) Solution set calculation of the Sun-perturbed optimal two-impulse trans-lunar orbits using continuation theory. *Astrodynamics* 4(1):75–86. <https://doi.org/10.1007/s42064-020-0069-6>
- He BY, Li HY, Zhang B (2013) Analysis of transfer orbit deviation propagation mechanism and robust design for manned lunar landing. *Acta Phys Sin-Ch Ed* 62(19):81–88. <https://doi.org/10.7498/aps.62.190505>
- He BY, Li HN, Zheng AW (2019) Adaptive LEO-phase free-return orbit design method for manned lunar mission based on LEO rendezvous. *J Astronaut Sci* 66(4):446–459. <https://doi.org/10.1007/s40295-019-00182-3>
- Komendera E, Scheeres D, Bradley E (2012) Intelligent computation of reachability sets for space mission. In: Proceedings of the Twenty-Sixth AAAI Conference on Artificial Intelligence. Toronto, Ontario, Canada
- Lee S, Hwang I (2018) Reachable set computation for spacecraft relative motion with energy-limited low-thrust. *Aerosp Sci Technol* 77(6):180–188. <https://doi.org/10.1016/j.ast.2018.02.034>
- Lee D, Butcher EA, Sanyal AK (2014) Optimal interior Earth-Moon Lagrange point transfer trajectories using mixed impulsive and continuous thrust. *Aerosp Sci Technol* 39(12):281–292. <https://doi.org/10.1016/j.ast.2014.09.016>
- Li HN (2014) Geostationary satellites collocation. Springer, Berlin, Heidelberg
- Li XH, He XS, Zhong QF (2011) Reachable domain for satellite with two kinds of thrust. *Acta Astronaut* 68(11–12):1860–1864. <https://doi.org/10.1016/j.actaastro.2011.01.004>
- Li JY, Gong SP, Wang X (2015) Analytical design methods for determining Moon-to-Earth trajectories. *Aerosp Sci Technol* 40:138–149. <https://doi.org/10.1016/j.ast.2014.10.016>
- Lu P, Xue SB (2010) Rapid generation of accurate entry landing footprints. *J Guid Control Dyn* 33(3):756–765. <https://doi.org/10.2514/1.46833>
- Mohammad S, Roberto CD (2019) Search-based method optimization applied to bi-impulsive orbital transfer. *Acta Astronaut* 161(8):389–404. <https://doi.org/10.1016/j.actaastro.2019.03.015>
- Peng QB, Shen HX, Li HY (2011) Free return orbit design and characteristics analysis for manned lunar mission. *Sci China Technol Sci* 54(12):3243–3250. <https://doi.org/10.1007/s11431-011-4622-7>
- Song Y, Song YJ, Kim KS et al (2020) Optimal lunar point return orbit design and analysis via a numerical three-step approach. *Int J Aeronaut Space Sci* 21:1129–1146. <https://doi.org/10.1007/s42405-020-00282-7>
- Stanley D, Cook S, Connolly J (2005) NASA's exploration system architecture study. NASA Report. No. TM-2005-214062.
- Wen CX, Peng C, Gao Y (2018) Reachable domain for spacecraft with ellipsoidal delta-v distribution. *Astrodynamics* 2(3):265–288. <https://doi.org/10.1007/s42064-018-0025-x>
- Wilson SW (1970) A pseudo-state theory for the approximation of three body trajectories. AAS/AIAA Astrodynamics conference, Santa Barbara, California. AIAA Paper. No. 70–1061. <https://doi.org/10.2514/6.1970-1061>
- Yan H, Gong Q (2011) High-accuracy trajectory optimization for a trans-earth-lunar mission. *J Guid Control Dyn* 34(4):1219–1227. <https://doi.org/10.2514/1.49237>
- Yang Z, Luo YZ, Zhang J (2019) Nonlinear semi-analytical uncertainty propagation of trajectory under impulsive maneuvers. *Astrodynamics* 3(1):61–77. <https://doi.org/10.1007/s42064-018-0036-7>
- Zhang G, Cao XB, Ma GF (2013) Reachable domain of spacecraft with a single tangent impulse considering trajectory safety. *Acta Astronaut* 91(10–11):228–236. <https://doi.org/10.1016/j.actaastro.2013.06.016>
- Zhou WM, Li HY, He BY (2019) Fixed-thrust Earth-Moon free return orbit design based on a hybrid multi-conic method of pseudo-perilune parameters. *Acta Astronaut* 160(7):365–377. <https://doi.org/10.1016/j.actaastro.2019.04.034>

Publisher's Note

Springer Nature remains neutral with regard to jurisdictional claims in published maps and institutional affiliations.

Submit your manuscript to a SpringerOpen[®] journal and benefit from:

- Convenient online submission
- Rigorous peer review
- Open access: articles freely available online
- High visibility within the field
- Retaining the copyright to your article

Submit your next manuscript at ► [springeropen.com](https://www.springeropen.com)